ISBN: 978-3-95450-232-5 ISSN: 2673-7000 doi:10.18429/JACoW-NAPAC2022-TUPA83

DERIVATIVE-FREE OPTIMIZATION OF MULTIPOLE FITS TO EXPERIMENTAL WAKEFIELD DATA

N. Majernik*, W. Lynn, G. Andonian, J. B. Rosenzweig, UCLA, Los Angeles, CA, USA
T. Xu, P. Piot, Northern Illinois University, DeKalb, IL, USA

Abstract

A method to reconstruct the transverse self-wakefields acting on a beam, based only on screen images, is introduced. By employing derivative-free optimization, the relatively high-dimensional parameter space can be efficiently explored to determine the multipole components up to the desired order. This technique complements simulations, which are able to directly infer the wakefield composition. It is applied to representative simulation results as a benchmark and also applied to experimental data on skew wake observations from dielectric slab structures.

INTRODUCTION

Transverse self-wakefields are an important consideration in many facets of beam physics, arising in dielectric, metallic, and plasma structures. In some instances, they may be desirable and intentionally excited, e.g. streakers [1], but in others they may lead to beam breakup [2, 3]. Due to their small spatial and temporal scales and synchronization with a relativistic beam, it can be difficult to directly measure these wakefields. It can be possible to make certain inferences about the wakefields based on the frequency content of the outcoupled wakefields [3, 4] or by comparing experimental measurements to simulations to check for agreement, but a method to more directly determine the fields would be desirable. Other techniques have been proposed including tailored witness beams [5], but in this work we introduce a technique for estimating the self-wakefields without requiring any novel hardware.

It is possible do describe the transverse wakefields, $\boldsymbol{W}$, at each longitudinal position along the beam with the standard multipole convention [6]:

$$A + iV = \sum_{n=1}^{\infty}(a_n + ib_n)(x + iy)^n; \boldsymbol{W} = -\left\{\frac{\partial V}{\partial x}, \frac{\partial A}{\partial x}\right\}, \quad (1)$$

where a_n and b_n are the n^{th} skew and normal multipole coefficients respectively. In this work, we make a thin lens approximation, *i.e.* that the beam's spatial distribution does not change over the the length of the wakefield interaction and that the structure is longitudinally invariant. We will further assume that the wakefield at every longitudinal location is equal, up to a multiplicative constant, $\kappa(z)$. Provided that the beam's length is short compared to the wavelength of all modes which appreciably contribute to the overall wakefield, this is a reasonable approximation; it will be further justified below.

* NMajernik@g.ucla.edu

TRANSVERSE WAKEFIELD RECONSTRUCTION

The technique takes as input two scintillator screen images, taken by the same screen, downstream of the wakefield interaction point; one with the structure in place and one without. These images are used as probability distribution functions (PDF) which are sampled to create two populations of n (x, y) points. A 2D grid of bins is defined that covers either beam, but with a bin spacing low enough to resolve the structure of the beams. The with-structure points are binned, yielding bin-wise counts $B_{i,j}$. The without-structure points are then transformed according to $(x, y) + (x_c, y_c) + \kappa\mathbf{W}$ where (x_c, y_c) are corrections for beam drift between the without-structure and with-structure shots (omitted for simulations where this effect is not present) and κ is the wakefield amplitude scale factor, sampled independently from the probability distribution function of the random variable $\mathcal{K}$. These transformed points are binned, yielding $\widetilde{B}_{i,j}$. We then define the overall error as $\sum|\widetilde{B}_{i,j} - B_{i,j}|/n$. A numerical optimizer is employed to minimize this error term by finding the best parameter vector $\{x_c, y_c, \mathcal{K}_1, \mathcal{K}_2, ..., a_1, b_1, a_2, b_2, ...\}$ where $\mathcal{K}_1, \mathcal{K}_2, ...$ are free parameters that define the PDF of $\mathcal{K}$, with multipole coefficients a_i, b_i up to the selected order.

This random variable $\mathcal{K}$ results from weighting the probability of the wakefield strength at a longitudinal position, $\kappa(z)$, by the current at that position, $I(z)$. Depending on the available information and the expected complexity, different definitions for the PDF may be used. For the simulated cases below, the values of $\kappa(z)$ and $I(z)$ can be found directly and used to construct the PDF. For experiments for which there are trusted simulations, this approach may be used. However, it is also possible to use less prior knowledge. For the experimental reconstructions below, a PDF with one optimizer parameter, $\mathcal{K}_1$, was used. If this does not give satisfactory results, it is possible to define the distribution based on other assumptions or with a greater number of free parameters.

Several methods were attempted for optimization in this relatively high dimensional parameter space. Derivative-based optimizers struggled due to the discontinuous and noisy nature of the data, resulting from binning discrete particles. Bayesian optimization worked better, but the comparatively high overhead of this technique made it suboptimal. The best performance was found using derivative-free [7], global optimization, especially differential evolution. This approach is not guaranteed to arrive at the actual wakefields, but since wakefields are often dominated by a few, low degree multipole components, it will often arrive at a good approximation.

ISBN: 978-3-95450-232-5 ISSN: 2673-7000 doi:10.18429/JACoW-NAPAC2022-TUPA83

BENCHMARKING TO SIMULATION

A dielectric wakefield particle-in-cell simulation was run in CST [8]. In this scenario, a beam with a charge of 1.95 nC, bunch length σ_z = 640 µm, aspect ratio 7.72:1 σ_x:σ_y, and a tilt of 2.19° (see Fig. 1) was run past an alumina slab 5 mm thick and 15 cm long, coated on the side opposite the beam with a layer of metal. This simulation corresponded to a skew wake experiment at AWA [9] with the exception that the simulated beam energy was 500 MeV to freeze the motion of the beam during the interaction to ensure the validity of the thin lens assumption. The transverse momenta of each particle was recorded before and after the interaction and used to construct an interpolated function for the wakefield $\boldsymbol{W}_{\mathrm{CST}}(x, y, z)$, taken to be the ground truth.

Subsequently, $\boldsymbol{W}_{\mathrm{CST}}(x, y, z)$ was sampled at a number of z slices, spaced with $\Delta z \ll \sigma_z$. These fields were then fit with the best $\boldsymbol{W}_{\mathrm{guess}}$ by finding the vector $\boldsymbol{c}_{\mathrm{slice}} = \{a_1, b_1, a_2, b_2, ..., a_n, b_n\}$ which minimizes

$$\mathrm{mean}\left(\frac{\left|\boldsymbol{W}_{\mathrm{CST}}(x_k, y_k, z_{\mathrm{slice}}) - \boldsymbol{W}_{\mathrm{guess}}(x_k, y_k)\right|}{\left|\boldsymbol{W}_{\mathrm{CST}}(x_k, y_k, z_{\mathrm{slice}})\right|}\right), \quad (2)$$

where k counts along the simulation macroparticles. In this case, coefficients up to $n = 6$ (dodecapole) were used. All of the errors from these fits were weighted according to the currents, $I(z_{\mathrm{slice}})$, and the mean relative error of the multipole fits was 12.6%. Fitting to higher degrees will yield lower errors.

To find the *aggregate multipole* coefficients, $\boldsymbol{c}_{\mathrm{agg}}$, calculate the average of all the $\boldsymbol{c}_{\mathrm{slice}}$ vectors, weighted by the current at that longitudinal position, $I(z_{\mathrm{slice}})$. These coefficients, via Eq. (1), yield the aggregate wakefield $\boldsymbol{W}_{\mathrm{agg}}$. As previously discussed, we assume that the fields at every slice are equal to the aggregate wakefield, with a multiplicative constant: $\boldsymbol{c}_{\mathrm{slice}} = \kappa(z) * \boldsymbol{c}_{\mathrm{agg}}$. This is a reasonable approximation if the wavelengths of modes which produce relevant multipoles are long relative to σ_z, which is valid for scenarios under consideration. In Fig. 2, the normalized coefficients for the first three multipole moments are shown as a function of z; since the curves are the same shape, this supports the use of this approximation. At each slice, $\kappa(z)$ was calculated. The relative difference between the slice's 6$^{\mathrm{th}}$ order decomposition and $\boldsymbol{W}_{\mathrm{agg}}\kappa(z_{\mathrm{slice}})$ was weighted by by $I(z_{\mathrm{slice}})$, and the overall mean relative error was 3.1%: further evidence that the longitudinal approximation was valid.

The PDF for the wakefield strength was constructed using these results. Finally, to determine the overall quality of all these approximations, we calculate:

$$\mathrm{mean}\left(\frac{\left|\boldsymbol{W}_{\mathrm{CST}}(x_k, y_k, z_k) - \kappa(z_k)\boldsymbol{W}_{\mathrm{agg}}(x_k, y_k)\right|}{\left|\boldsymbol{W}_{\mathrm{CST}}(x_k, y_k, z_k)\right|}\right), \quad (3)$$

where k counts along the simulation macroparticles. This yields an overall error of 13%, suggesting that an approximation to 6$^{\mathrm{th}}$ order and limited longitudinal dependence is reasonable for this case.

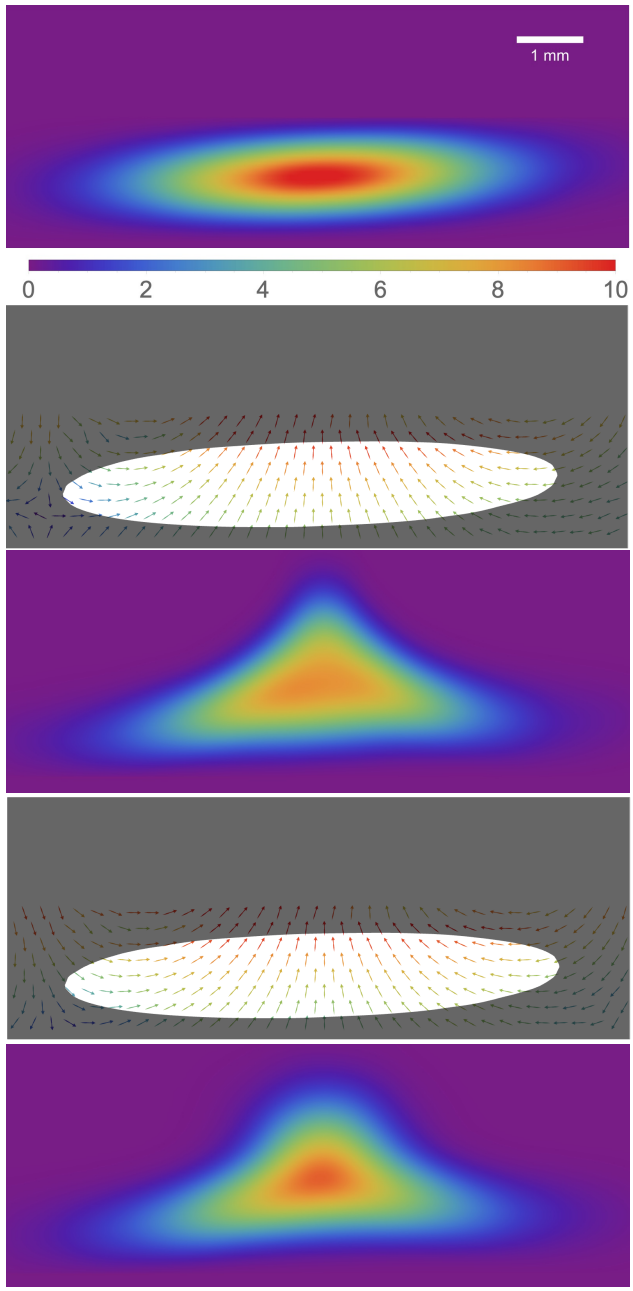

Figure 1: **First** Transverse profile of without-structure CST beam. (Plot range is constant for all subfigures. Charge density [Arb. units] color scale bar is constant between distributions). **Second** Reconstructed wakefields, $\boldsymbol{W}_{\mathrm{opt}}$. White region contains 90% of beam charge. **Third** Implied final, with-structure beam distribution by $\boldsymbol{W}_{\mathrm{opt}}$. **Fourth** Ground truth wakefields, $\boldsymbol{W}_{\mathrm{agg}}$. **Fifth** Ground truth final, with-structure beam distribution.

Simulated screen images were produced from the simulation data and fed into the optimizer described in the previous section. In this case, the only free parameters were the multipole coefficients. Finally, these optimizer-derived multipole coefficients and resultant field, $\boldsymbol{W}_{\mathrm{opt}}$, were benchmarked

ISBN: 978-3-95450-232-5 ISSN: 2673-7000 doi:10.18429/JACoW-NAPAC2022-TUPA83

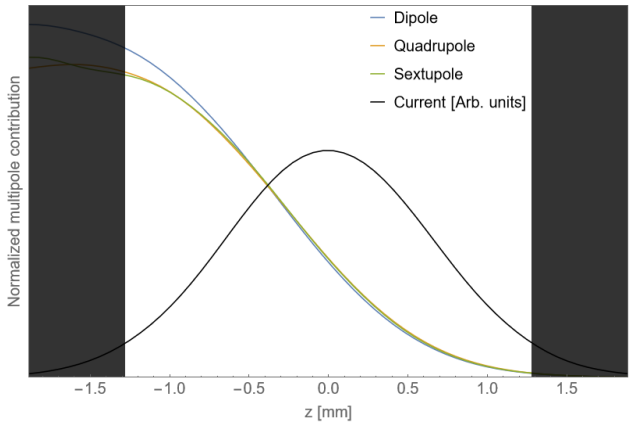

Figure 2: At each longitudinal position along the beam, a multipole decomposition was performed. For the first three orders, the values of $\sqrt{a_i^2 + b_i^2}$ are shown, after being normalized to the same scale (in reality, certain orders may have much more influential effects on the overall field). Also shown is the current profile of the beam, with the white region near the center corresponding to 90% of the beam charge.

against the ground truth using:

$$\text{median}\left(\frac{\left|\boldsymbol{W}_{\text{agg}}(x_k, y_k) - \boldsymbol{W}_{\text{opt}}(x_k, y_k)\right|}{\left|\boldsymbol{W}_{\text{agg}}(x_k, y_k)\right|}\right), \qquad (4)$$

yielding a relative error for the reconstruction of 11%.

REAL WORLD DATA

This technique has also been applied to experimental data. In Fig. 3, a dielectric wakefield interaction at AWA has been reconstructed to 6$^{\text{th}}$ order. This effort is discussed in much greater detail in [9] where the reconstructed wakefields are compared to both simulations and analytic models of the skew wake interaction. In this case, the PDF of $\mathcal{K}$ had one free parameter and was given by $f_{\mathcal{K}}(\kappa) = (1 + \mathcal{K}_1)\kappa^{\mathcal{K}_1}$ for $0 < \kappa < 1$. x_c and y_c were also varied, for a total parameter space dimension of 15.

DISCUSSION

We have introduced a technique for reconstructing the transverse self-wakefields of a beam without additional hardware. The approach has been benchmarked against simulations where the simulated fields may serve as a ground truth to quantify the accuracy of the technique. This technique has also been applied to experimental data, with comparisons to simulation and theory published elsewhere [9].

In the future, we will continue to extend, refine, and quantify this technique. The goodness of fit for reconstructions of higher degree multipoles will be determined. Additionally, we will extend the technique to explicitly account for the effects of a beam that evolves spatially during the wakefield interaction. Also, we will reconstruct simulation wakefields using various forms of the $\mathcal{K}$ PDF and compare to the idealized case shown here. Finally, we will consider using data from multiple screens to further refine the reconstruction.

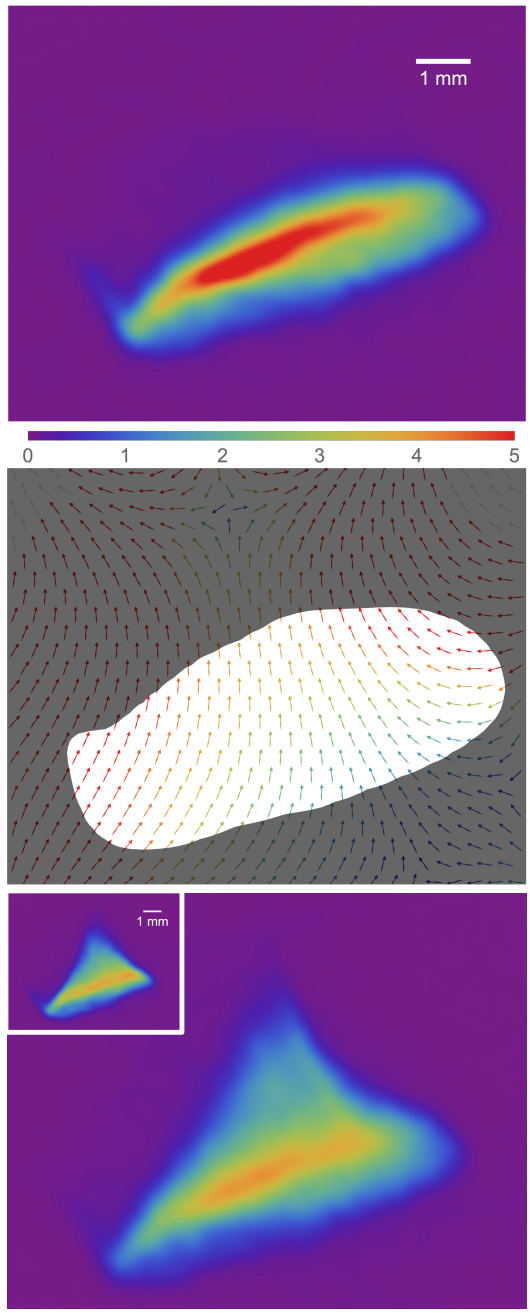

Figure 3: **First** Transverse profile of without-structure, AWA beam. (Plot range is constant for all subfigures. Charge density [Arb. units] color scale bar is constant between distributions). **Second** Reconstructed wakefields, $\boldsymbol{W}_{\text{opt}}$. White region contains 90% of beam charge. **Third** Implied final, with-structure beam distribution by $\boldsymbol{W}_{\text{opt}}$. **Inset** Ground truth with-structure beam distribution, from experiment.

This work was supported by DOE Grant No. DE-SC0017648. TX and PP are supported by DOE Grant No. DE-SC0018656.

ISBN: 978-3-95450-232-5 ISSN: 2673-7000 doi:10.18429/JACoW-NAPAC2022-TUPA83

REFERENCES

[1] S. Bettoni *et al.*, "Temporal profile measurements of relativistic electron bunch based on wakefield generation", *Physical Review Accelerators and Beams*, vol. 19, no. 2, p. 021304, 2016. doi:10.1103/PhysRevAccelBeams.19.021304

[2] C. Li *et al.*, "High gradient limits due to single bunch beam breakup in a collinear dielectric wakefield accelerator", *Physical Review Special Topics-Accelerators and Beams*, vol. 17, no. 9, p. 091302, 2014. doi:10.1103/PhysRevSTAB.17.091302

[3] B. D. O'Shea *et al.*, "Suppression of deflecting forces in planar-symmetric dielectric wakefield accelerating structures with elliptical bunches", *Physical Review Letters*, vol. 124, no. 10, p. 104801, 2020. doi:10.1103/PhysRevLett.124.104801

[4] N. Majernik *et al.*, "Positron driven high-field terahertz waves via dielectric wakefield interaction", *Physical Review Research*, vol. 4, no. 2, p. 023065, 2022. doi:10.1103/PhysRevResearch.4.023065

[5] A. Halavanau, S. J. Gessner, C. E. Mayes, and J. B. Rosenzweig, "Hollow and Flat Electron Beam Generation at FACET-II", in *Proc. 12th Int. Particle Accelerator Conf. (IPAC'21)*, Campinas, Brazil, May 2021, pp. 376-378. doi:10.18429/JACoW-IPAC2021-MOPAB101

[6] J. T. Tanabe, *Iron dominated electromagnets: design, fabrication, assembly and measurements*. New York, NY, USA: World Scientific, 2005. doi:10.1142/5823

[7] S. Koziel and X. S. Yang, eds. *Computational optimization, methods and algorithms*. New York, NY, USA: Springer, 2011. doi:10.1007/978-3-642-20859-1

[8] CST studio suite (electromagnetic field simulation software): https://www.3ds.com/products-services/simulia/products/cststudio-suite/.

[9] W. Lynn *et al.*, "Observation of Skewed Electromagnetic Wakefields in an Asymmetric Structure Driven by Flat Electron Bunches", to be published.